

# Improving Performance of Sensor less Brushless DC Motor Drive using ANFIS Back-EMF Observer

B.V. ARUN KUMAR\*, Dr .G V MARUTHESWAR\*\*

\* Research Scholar, \*\* professor, Department of Electrical and Electronics Engineering, Sri Venkateswara University College of Engineering, SV University, Tirupati, Andhrapradesh, India.

**Abstract** - The BLDC motor has advantages of the DC motor such as simple control, high torque, high efficiency and compactness. Also, brush maintenance is no longer required, and many problems resulting from mechanical wear of brushes and commutators are improved by changing the position of rotor and stator in DC motor. However, the problems for the cost and reliability of rotor position sensors have motivated research in the area of position sensorless BLDC motor drives. In recent years, many sensorless drive methods have been proposed for improving the performance of BLDC motors without a position sensor.

This project presents the ANFIS back-EMF observer based on fuzzy inference system and back propagation algorithm and a novel sensorless control algorithm using this observer. ANFIS reacts faster in adjusting the speed of dc motor to achieve the desired speed when compared with other sensorless drive methods. so the settling time of the rotor speed using ANFIS controller is less when compared with other controller and the commutation signal shows good performance.

**Keywords:** BLDC Motor, Back Emf observer, PI, FUZZY, ANFIS Controllers

## I. INTRODUCTION

Brushless DC electric motor (BLDC motors, BL motors) also known as electronically commutated motors (ECMs, EC motors) are synchronous motors that are powered by a DC electric source via an integrated inverter/switching power supply, which produces an AC electric signal to drive the motor. In this context, AC, alternating Current, does not imply a sinusoidal waveform, but rather a bi-directional current with no restriction on waveform. Additional sensors and electronics control the inverter output Amplitude and waveform (and therefore percent of DC bus usage/efficiency) and frequency (i.e. rotor speed).

The rotor part of a brushless motor is often a permanent magnet synchronous motor, but can also be a switched reluctance motor, or induction motor.

## II. MATHEMATICAL MODEL OF BLDC MOTOR DRIVE SYSTEM

This chapter discusses about the BLDC motor drive system, three phase voltage source inverter, system state equations of the BLDC motor and the block diagram of back-EMF observer obtained by these system state equations after an observer is added to the system.

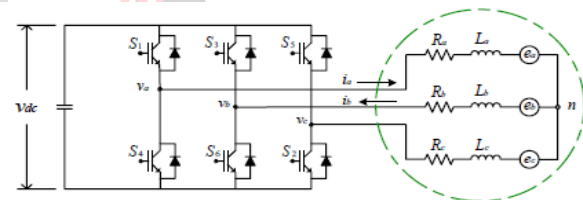


Fig 1. Three phase inverter BLDC motor

## III. THREE PHASE VOLTAGE SOURCE INVERTER

A three-phase inverter converts a DC input into a three-phase AC output. Its three arms are normally delayed by an angle of  $120^\circ$  so as to generate a three-phase AC supply. The inverter switches each has a ratio of 50% and switching occurs after every  $T/6$  of the time  $T$  ( $60^\circ$  angle interval). The switches  $S1$  and  $S4$ , the switches  $S2$  and  $S5$  and switches  $S3$  and  $S6$  complement each other.

The figure below shows a circuit for a three phase inverter. It is nothing but three single phase inverters put across the same DC source. The pole voltages in a three phase inverter are equal to the pole voltages in single phase half bridge inverter.

The two types of inverters above have two modes of conduction  $180^\circ$  mode of operation and  $120^\circ$  degree mode of operation.  $120^\circ$  degree mode of operation is used in BLDC motor.

## 120 DEGREE CONDUCTION MODE

TABLE 1 Switching of 120 degree conduction mode

Mode	S1	S2	S3	S4	S5	S6
1 <sup>st</sup>	ON	OFF	OFF	OFF	OFF	ON
2 <sup>nd</sup>	ON	ON	OFF	OFF	OFF	OFF
3 <sup>rd</sup>	OFF	ON	ON	OFF	OFF	OFF
4 <sup>th</sup>	OFF	OFF	ON	ON	OFF	OFF
5 <sup>th</sup>	OFF	OFF	OFF	ON	ON	OFF
6 <sup>th</sup>	OFF	OFF	OFF	OFF	ON	ON

For the 120° degree mode VSI, each thyristor conducts for 120° of a cycle. Like 180° mode, 120° mode inverter also requires six steps, each of 60° duration for completing one cycle output AC voltage. A table 1 giving the sequence of firing the six thyristor is prepared as shown in the top. In this table, shown that even conducts for 120° and for the next 60° neither S1 nor S4 conducts. Now S4 is turned on at  $\omega t=180^\circ$  is further conducts for 120°, i.e. from  $\omega t=180^\circ$  to at  $\omega t=300^\circ$ . This means that for 60° interval from  $\omega t=120^\circ$  to  $\omega t=180^\circ$ , series connected switch S1, S4 do not conduct. At  $\omega t=300^\circ$ , S4 is turned off, then 60° interval elapses before S1 is turned on again at  $\omega t=360^\circ$ . In the second row, S3 is turned on at  $\omega t=120^\circ$  as in 180° mode inverter. Now S3 conducts for 120°, then 60° interval elapses during which neither S3 nor S6 conducts. At  $\omega t=300^\circ$ , S6 is turned on, it conducts for 120° and then 60° interval elapses after which S3 is turned on again. The third row is also completed similarly. This table shows that S6, S1 should be gated for step I; S1, S2 for step II; S2, S3 for step III and so on. The sequence of firing the six thyristor is the same as for the 180 mode inverter. During each step, only two thyristors conduct for this inverter one from the upper group and one from the lower group; but in 180° mode inverter, three thyristors conduct in each step.

The individual phase equations of electrical equivalent circuit of BLDC motor can be written as follows

$$V_a = i_a R_a + L_a \frac{d}{dt} i_a + e_a \quad (3.1)$$

$$V_b = i_b R_b + L_b \frac{d}{dt} i_b + e_b \quad (3.2)$$

$$V_c = i_c R_c + L_c \frac{d}{dt} i_c + e_c \quad (3.3)$$

where  $R_a, R_b, R_c$  are phase resistances,  $L_a, L_b, L_c$  are phase inductances,  $V_a, V_b, V_c$  are phase voltages,  $i_a, i_b, i_c$  are phase currents and  $e_a, e_b, e_c$  are phase back emf's. Therefore, assuming that self and mutual inductances are constant, the voltage equation of three phases is given by

$$\begin{bmatrix} V_a \\ V_b \\ V_c \end{bmatrix} = \begin{bmatrix} R_a & 0 & 0 \\ 0 & R_b & 0 \\ 0 & 0 & R_c \end{bmatrix} \begin{bmatrix} i_a \\ i_b \\ i_c \end{bmatrix} + \begin{bmatrix} L_a & 0 & 0 \\ 0 & L_b & 0 \\ 0 & 0 & L_c \end{bmatrix} \frac{d}{dt} \begin{bmatrix} i_a \\ i_b \\ i_c \end{bmatrix} + \begin{bmatrix} e_a \\ e_b \\ e_c \end{bmatrix} \quad (3.4)$$

The torque equation is given by

$$T_e = \frac{e_a \cdot i_a + e_b \cdot i_b + e_c \cdot i_c}{\omega_m} \quad (3.5)$$

Where  $T_e$  is the obtained torque and  $\omega_m$  is the rotor speed.

Subtracting (3.2) from (3.1), the line to line voltage  $V_{ab}$  is found as

$$V_{ab} = V_a - V_b = (i_a - i_b) R_s + L \frac{d}{dt} (i_a - i_b) + (e_a - e_b) \quad (3.6)$$

From (3.6), the back EMF difference can be found as

$$e_a - e_b = (V_a - V_b) - (i_a - i_b) R_s - L \frac{d}{dt} (i_a - i_b) \quad (3.7)$$

Subtracting (3.3) from (3.2) leads to another equation as follows:

$$e_b - e_c = (V_b - V_c) - (i_b - i_c) R_s - L \frac{d}{dt} (i_b - i_c) \quad (3.8)$$

Subtracting (3.1) from (3.3) leads to another equation as follows:

$$e_c - e_a = (V_c - V_a) - (i_c - i_a) R_s - L \frac{d}{dt} (i_c - i_a) \quad (3.9)$$

Taking  $e_a - e_b = e_{ab}$ ,  $e_b - e_c = e_{bc}$ ,  $e_c - e_a = e_{ca}$ ,  $V_a - V_b = V_{ab}$  and  $V_b - V_c = V_{bc}$ ,

$$V_{ca} = V_c - V_a$$

the following equations can be written:

$$e_{ab} = V_{ab} - (i_a - i_b) R_s - L \frac{d}{dt} (i_a - i_b) \quad (3.10)$$

$$e_{bc} = V_{bc} - (i_b - i_c) R_s - L \frac{d}{dt} (i_b - i_c) \quad (3.11)$$

$$e_{ca} = V_{ca} - (i_c - i_a) R_s - L \frac{d}{dt} (i_c - i_a) \quad (3.12)$$

It is found that at any 60° commutation period, only two of the phases are energized and the other phase current remains zero. Moreover, one of the conducting phase current is 180° out of phase with the other conducting phase. That simply means, one of the phase currents is entering to the neutral and the other is leaving neutral.

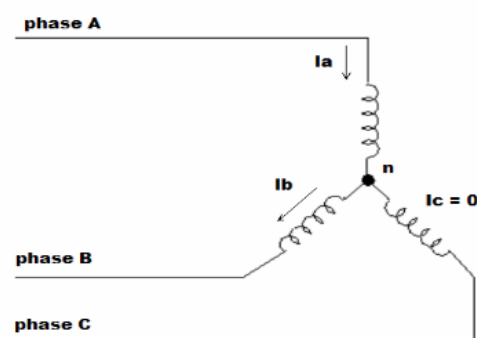


Fig 2 Typical BLDC motor phase excitation at a particular instant

Assuming a balanced three phase system and peak value of the phase currents same ( $i_a = i_b = i_c = i$ ), the total current flowing through the motor at any commutation instant becomes  $i_a - (-i_b) = 2*i = 2*i_{ab}$ , where  $i_{ab} = i$ .

This value when used in equation (3.8) gives

$$V_{ab} = 2i_{ab} R_s + 2L_s \frac{d}{dt} i_{ab} + e_{ab} \quad (3.13)$$

Rearranging (3.11), we get equation (3.12),

$$\frac{di_{ab}}{dt} = -\frac{2R_s}{2L_s}i_{ab} - \frac{1}{2L_s}e_{ab} + \frac{1}{2L_s}v_{ab} \quad (3.14)$$

Since the neutral point of the BLDC motor is unknown when manufactured, this observer is considered by the equation (3.12), where  $i_{ab}$  and  $v_{ab}$  can be measured, that is why they are called known state variables. But  $e_{ab}$  cannot be measured so it is referred as unknown state variable. Equation (3.12) can be written as

$$\dot{x} = Ax + Bu + Dv \quad (3.15)$$

$$y = Cx \quad (3.16)$$

where,  $A = [-\frac{2R_s}{2L_s}]$ ,  $B = [\frac{1}{2L_s}]$ ,  $D = [\frac{-1}{2L_s}]$ ,  $x = [i_{ab}]$ ,  $u = [v_{ab}]$ ,  $v = [e_{ab}]$ ,  $y = [i_{ab}]$ ,  $C = [1]$ .

The back EMF here is considered as unknown disturbance. Typically, unknown disturbances can be represented by differential equations. Since no experimental data is available for disturbance, the unknown disturbance is modeled by the general completely observable dynamic system. Then the entire system can be represented by an augmented equation that models the back EMF in the form of a differential equation. The augmented model is described by the following equations:

$$\dot{x} = Ax + Bu \quad (3.17)$$

$$y = Cx \quad (3.18)$$

where  $A = [\frac{-2R_s}{2L_s} \quad \frac{-1}{2L_s}]$ ;  $B = [\frac{1}{2L_s}]$ ;  $x = [\begin{matrix} i_{ab} \\ e_{ab} \end{matrix}]$ ;  $u = [v_{ab}]$ ,  $y = [i_{ab}]$ ,  $C = [1 \ 0]$ ;

The observability matrix of this system described by

(3.17) and (3.18) is  $[\begin{matrix} 1 & 0 \\ \frac{2R_s}{2L_s} & \frac{-1}{2L_s} \end{matrix}]$ , which has a rank of 2. So

it can be safely stated that the system is completely observable, and a state observer can be added to the system.

The following observer is composed for the system:  $\hat{x}$

$$= Ax + Bu + K(y - \hat{y}) \quad (3.19)$$

Where  $\hat{x}$  is the observed value of the state variables and  $\hat{y}$  is the observed value of the output which, in this case, is the line to line current.  $K$  is the gain matrix for the observer and it can be chosen carefully in a trial and error basis or by solving it. Careful selection of  $K$  can lead to accurate estimation of the line to line back EMF of the motor.

## IV. CONTROLLERS

### 4.1 PI CONTROLLER

#### 4.1.1 PROPORTIONAL RESPONSE

The proportional component depends only on the difference between the set point and the process variable.

This difference is referred to as the Error term. The proportional gain  $K$  determines the ratio of output response to the error signal. For instance, if the error term has a magnitude of 10, a proportional gain of 5 would produce a proportional response of 50. In general, increasing the proportional gain will increase the speed of the control system response. However, if the proportional gain is too large, the process variable will begin to oscillate. If  $K$  is increased further, the oscillations will become larger and the system will become unstable and may even oscillate out of control.

#### 4.1.2 INTEGRAL RESPONSE

The integral component sums the error term over time. The result is that even a small error term will cause the integral component to increase slowly. The integral response will continually increase over time unless the error is zero, so the effect is to drive the Steady-State error to zero. Steady-State error is the final difference between the process variable and set point. A phenomenon called integral windup results when integral action saturates a controller without the controller driving the error signal toward zero.

PI controller will eliminate forced oscillations and steady state error resulting in operation of on-off controller and P controller respectively. However, introducing integral mode has a negative effect on speed of the response and overall stability of the system.

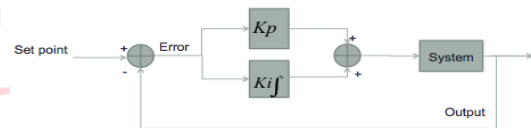


Fig 3. Block diagram of PI controller

The controller output in this case is :  $u(t) = K_p \cdot e(t) + K_i \int e(t) dt$

### 4.2 Fuzzy logic controller

Usually fuzzy logic control system is created from four major elements presented on Figure 2: fuzzification interface, fuzzy inference engine, fuzzy rule matrix and defuzzification interface.

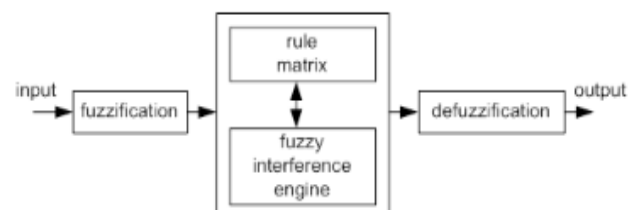


Fig 4 Fuzzy logic controller

The inputs given to the fuzzy logic controller are line to line current error of the BLDC motor and differential value

of the error. These inputs are given by

$$err(i_{ab}) = i_{ab} - \hat{i}_{ab} \quad (4.2)$$

$$cerr(i_{ab}) = err(i_{ab})(n-1) - err(i_{ab})n \quad (4.3)$$

Where line to line current error is the difference between measured value and actual value and change in the error is the difference between present error and previous error. The output obtained from the fuzzy logic controller is the change in back emf.

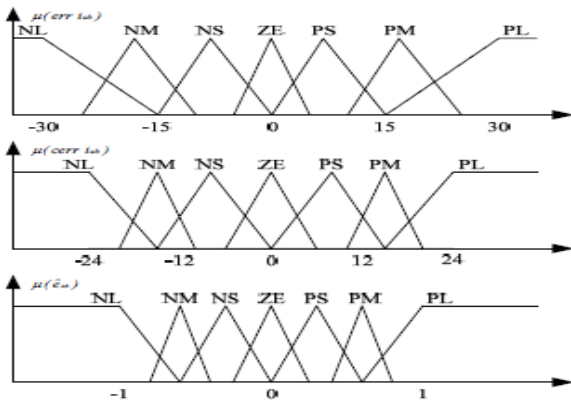


Fig 5. Membership functions of two input variables and one output variable

### 4.3 ADAPTIVE NEURO FUZZY INFERENCE SYSTEM

The concept of fuzzy logic and artificial neural network for control problem has been grown into a popular research topic in recent years. The reasons that the classical control theory usually requires a mathematical model for designing the controller. The inaccuracy of mathematical modeling of the plants usually degrades the performance of the controller, especially for nonlinear and complex control problems. The advent of the fuzzy logic controllers (FLC) and the neural controllers based on multilayered neural networks has inspired new resources for the possible realization of better and more efficient control. In recent years, the integration between fuzzy logic and neural network namely fuzzy neural network (FNN) has been proposed and developed; generally the combination of fuzzy logic and neural network is called as ANFIS (Adaptive Neuro Fuzzy Inference System). Neural system has many input and also has multiple outputs but the fuzzy logic has multiple inputs and single output, so the combination of this two is known as ANFIS which issued for nonlinear applications.

#### 4.3.1 IMPLEMENTATION OF ANFIS

Rule 1: If  $x$  is  $A_1$  and  $y$  is  $B_1$  Then  $f_1 = p_1x + q_1y + r_1$

Rule 2: If  $x$  is  $A_2$  and  $y$  is  $B_2$  Then  $f_2 = p_2x + q_2y + r_2$

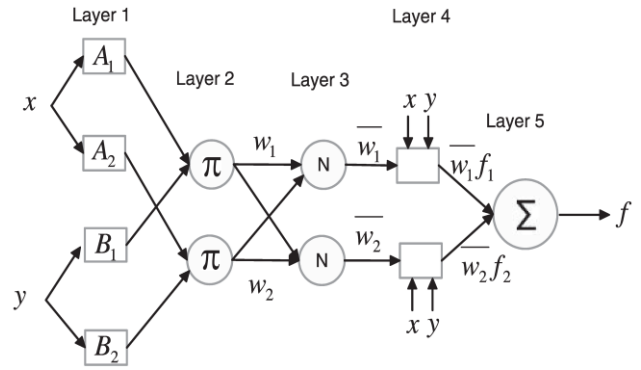


Fig:5 ANFIS structure for 2 input variables for TSK model

**Layer 1:** Every node  $i$  in this layer is a square node with anode function

$$O_{1,i} = \mu_{v,i}(v) \text{ for } i = 1, 2$$

$$O_{1,j} = \mu_{d,j}(v) \text{ for } j = 1, 2$$

Where  $x$  is the input to node 0, and  $A$  is the linguistic label function specifies the degree to which the given  $x$  satisfies the quantifier  $A_i$ . Gaussian Membership function is chosen with maximum equal to 1 and minimum equal to 0. Parameters in this layer are referred to as the premise parameters. Membership functions are used for each of the input in this layer[7].

**Layer 2:** Every node in this layer is a circle node labeled  $H$ , which multiplies the incoming signals and sends the product out. For instance,

$$O_{2,i} = w_i = \mu_{v,i}(v) \cdot \mu_{D_j}(d), \quad i = 1, 2$$

Each node output represents the firing strength of a rule

**Layer 3:** Every node in this layer is a circle node labeled  $N$ . The  $i$ -th node calculates the ratio of the  $i$ -th rule's firing strength to the sum of all rules' firing strengths

$$O_{3,i} = \bar{w}_i = \frac{w_i}{w_1 + w_2}, \quad i = 1, 2$$

For convenience, outputs of this layer will be called normalized firing strengths.

**Layer 4:** Every node 1 in this layer is a square node with anode function

$$O_{4,i} = \bar{w}_i f_i = \bar{w}_i (p_i v + q_i d + r_i), \quad i = 1, 2$$

Where  $\bar{w}_i$ , is the output of layer 3 and  $\{p_i, q_i, r_i\}$  is the parameter set. Parameters in this layer will be referred to as consequent parameters.

**Layer 5:** The single node in this layer is a circle node labeled  $E$  that computes the overall output as the summation of all incoming, signals, i.e.

$$O_{5,i} = \sum_i \bar{w}_i f_i = \frac{\sum_i w_i f_i}{w_1 + w_2}, \quad i = 1, 2$$

## V. COMMUTATION FUNCTION

The sensor less control method that decides commutation instances of switching devices by detecting ZCP of back-EMF has been commonly used. However, this method cannot detect ZCP at a low-speed range. In order to solve this problem, the sensitive commutation function defined by using the line-to-line back-EMF observer is proposed to improve the performance of the Sensorless control scheme as shown in Fig6 and the commutation functions (CF) are defined as below:

$$\text{Mode 1 and 4: } CF(\theta_1) = \frac{\hat{e}_{bc}}{\hat{e}_{ca}}, \quad (5.5)$$

$$\text{Mode 2 and 5 } CF(\theta_2) = \frac{\hat{e}_{ab}}{\hat{e}_{bc}}, \quad (5.6)$$

$$\text{Mode 3 and 6: } CF(\theta_3) = \frac{\hat{e}_{ca}}{\hat{e}_{ab}} \quad (5.7)$$

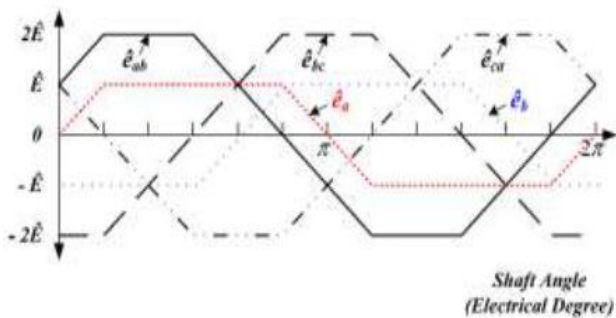


Fig 6 Relation between the estimated line to line back EMFs and estimated back EMFs

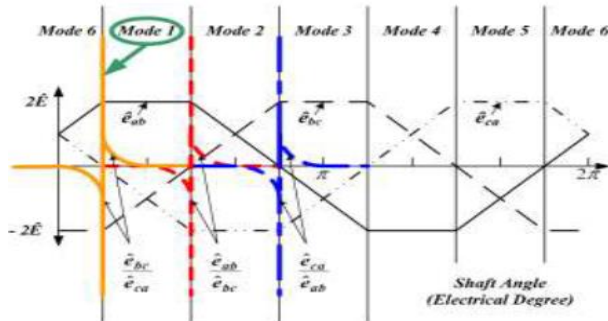


Fig 7 Proposed commutation functions

As shown in Fig7 , the commutation function for the mode conversion from mode 6 to 1 is represented by the fractional equation consisted of the numerator ( $\hat{e}_{bc}$ ) having a constant negative magnitude and the gradually decreasing denominator ( $\hat{e}_{ca}$ ). Before mode change, this commutation function instantaneously changes from negative infinity to positive infinity and this moment is considered as the position signal so that this feature can be certainly distinguished from noises by selecting a relevant threshold magnitude. Although the similar commutation function was already proposed[8],the proposed commutation function in this project is easy to decide the threshold of commutation function because it has a negative value before commutation. Also, since this commutation function is consisted of the estimated back-EMF, it is robust for noise.

## VI. RESULTS AND DISCUSSION

### 6.1 BACK-EMF DISTURBANCE MODEL USING ESTIMATED BACK-EMF

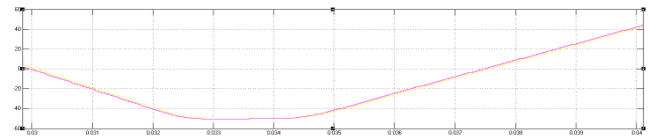


Fig 8 Line to line back-EMF (zoomed version)

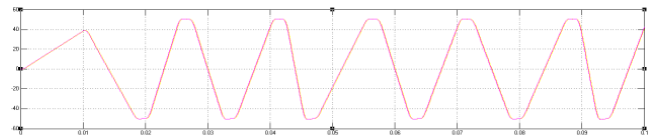


Fig 9 Extended line to line back-EMF

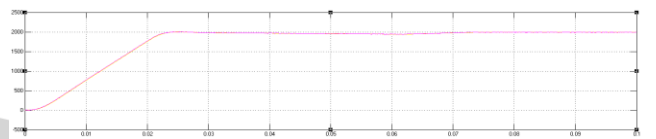


Fig 10 Rotor speed

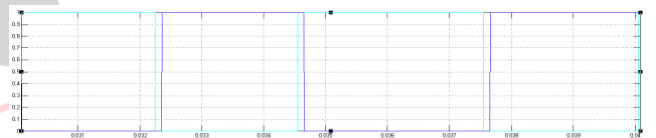


Fig 11 Commutation signal

These are the results of the back-EMF disturbance model using the estimated back-EMF. An estimation of constant back-EMF shows satisfied results as shown in Fig. 8 and Fig 9. But in the case of the back-EMF changes, the estimated value shows a delay. As a result, transient state of the rotor speed and the commutation signal has a delay as shown in Fig.10 and Fig 11.

### 6.2 BACK-EMF DISTURBANCE MODEL USING PI CONTROLLER

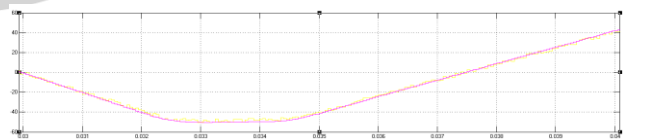


Fig 10 Line to line back-EMF using PI controller (zoomed version)

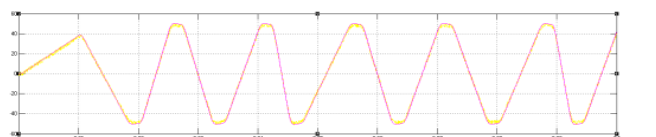


Fig 11 Extended line to line back-EMF using PI controller

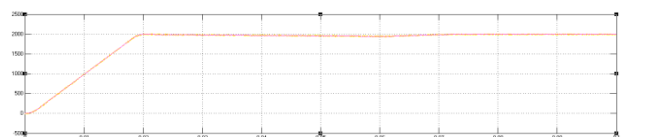


Fig 12 Rotor speed using PI controller

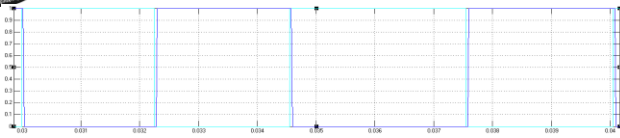


Fig 13 Commutation signal using PI controller

These are the results of the back-EMF disturbance model using the PI controller. Contrary to the case 1, an estimation of a changing back-EMF shows good performance. But in the case of constant back-EMF, ripples are present as shown in in Fig10 and Fig 11. As a result, the rotor speed on steady state has ripple as shown in Fig12. But the commutation signal shows high performance because an estimation of changed back-EMF is superior as shown in Fig 13.

### 6.3 BACK-EMF DISTURBANCE MODEL USING FUZZY LOGIC

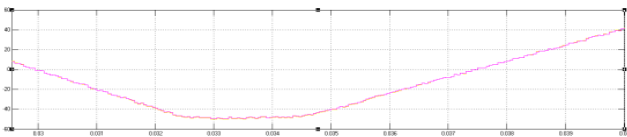


Fig 14 Line to line back-EMF using FUZZY controller (zoomed version)

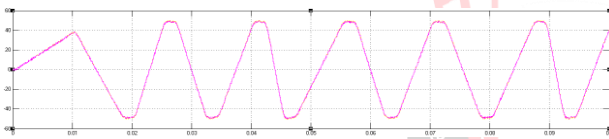


Fig 15 Extended line to line back-EMF using FUZZY controller

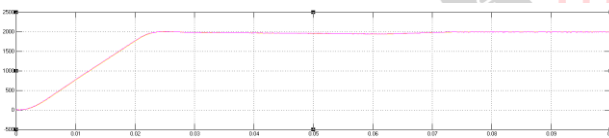


Fig 16 Rotor speed using FUZZY controller

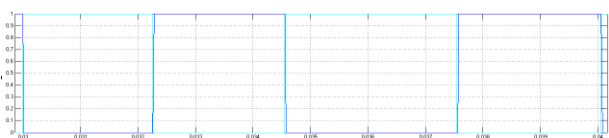


Fig 17 Commutation signal using FUZZY controller

These are the results of the fuzzy-back EMF observer to solve the problems of the above two cases. Because both constant and varying back-EMF shows good performance by using the fuzzy back-EMF observer as shown in Fig 14 and Fig 15. And the performance of both the rotor speed on entire states and the commutation signal shows superior performance when compared with observers using the back-EMF disturbance model in the previous two cases as shown in Fig 16 and Fig 17.

### 6.4 BACK-EMF DISTURBANCE MODEL USING ANFIS

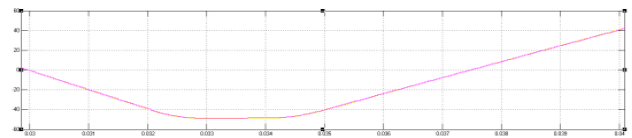


Fig 18 Line to line back-EMF using ANFIS controller (zoomed version)

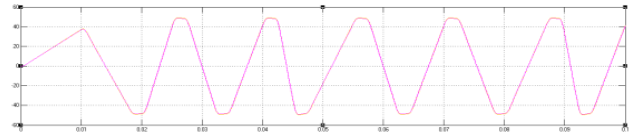


Fig 19 Extended line to line back-EMF using ANFIS controller

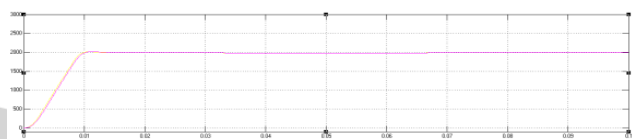


Fig 20 Rotor speed using ANFIS controller

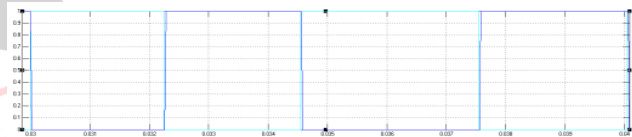


Fig 21 Commutation signal using ANFIS controller

These are the results of back-EMF disturbance model using ANFIS (adaptive neuro-fuzzy inference system). Both constant and changing back-EMF are excellently estimated by this observer as shown in Fig 18 and Fig 19, because ANFIS can estimate a variable shape function such as back-EMF of the BLDC motor. When compared to fuzzy controller, ANFIS controller reacts faster in adjusting the speed of dc motor to achieve the desired speed and ripples are further reduced using this ANFIS controller as shown in Fig 20. Thus the settling time of ANFIS controller is lower than fuzzy logic controller. Commutation signal shows superior performance as shown in Fig 21.

TABLE 6.3 Comparison of different parameters for controllers

Parameter	Estimated value	PI controller	FUZZY controller	ANFIS controller
Rise time	0.021	0.018	0.02	0.0085
Settling time	0.075	0.072	0.078	0.071
Percentage overshoot	0.9	1.1	0.95	0.9
Steady state error	-0.0005	0.0005	0.0005	0.0005

## VII. CONCLUSIONS

Conventional sensor less methods of the BLDC motor have low performance in transient state or low speed range and occasionally require additional circuit. Therefore, to

cope with this problem, ANFIS back-EMF observer is proposed using the commutation function by closed loop, so that it will continuously estimates a back-EMF of trapezoidal shape. Also, the proposed algorithm using this ANFIS back-EMF observer can achieve robust control for the change of an external condition and continuously estimate the speed of the rotor at transients as well as steady state. Fuzzy logic controller still perform well on controlling the speed of the DC motor where the controller manage to control the speed to follow the reference speed set by the controller. Thus the settling time of ANFIS controller is lower than fuzzy logic controller. The technical validity of the proposed algorithm has been shown through computer simulation using the Matlab.

### REFERENCES

- [1] P. Pillay and R. Krishnan, "Modeling, simulation and analysis of permanent-magnet motor drives, part-II: the brushless DC motor drives," IEEE Trans. on Industry Applications, vol. 25, pp.274-279, March/April 1989.
- [2] K. Naga Sujatha, K. Vaisakh and Anand. G. 2010. Artificial Intelligence based speed control of brushless DC motor. IEEE 978-1-4244-6551-4/10.
- [3] Krishnan R motor "Drives Modeling, Analysis and Control", Prentice Hall of India, First Edn, 2002, Chapter 9, pp 513-615..
- [4] Cheng-Tsung Lin, Chung-Wen Hung and Chih-Wen Liu. 2007. Fuzzy PI controller for BLDC motors considering Variable Sampling Effect. IEEE Industrial Electronics Society (IECON). Nov. 5-8, Taipei, Taiwan.
- [5] Vandana Govindan T.K, Anish Gopinath and S. Thomas. 2011. George 'DSP based Speed control of Permanent Magnet Brushless DC motor. IJCA Special Issue on Computational Science - New Dimensions and Perspectives NCCSE.
- [6] Zhen-Yu Zhao. 1993. Masayoshi Tomizuka and Satoru Isaka Fuzzy Gain Scheduling of PID controllers. IEEE transactions on systems, man and cybernetics. 23(5).
- [7] P. Pillay and R. Krishnan. 2002. Modelling simulation and analysis of a Permanent magnet brushless Dc motor drive. IEEE trans. Ind Applicat. 26: 124-129.
- [8] Chung-Wen Hung, Jen-Ta Su, Chih-Wen Liu, Cheng-Tsung Lin and Jih-Han Chen. 2010. Fuzzy Gain Scheduling PI controller for Sensorless four switches three phase BLDC motor. IEEE 978-1-4244-47831/10.



B.V. ARUN KUMAR received B.tech in Electrical and Electronics Engineering from RGM CET, Nandyal, M.Tech(power electronics) Degree in G. Pullareddy Engineering college, Kurnool, presently Research Scholar in Department of Electrical and Electronics Engineering, Sri Venkateswara University College of Engineering, SV University, Tirupati, Andhrapradesh, India-517502. Email: venkatarun206@gmail.com



Dr. G. V. MARUTHESWAR received B.tech, M.tech (Instrumentation and control engineering) & Ph.D Degree in Electrical and Electronics Engineering from, Sri Venkateswara University College of Engineering, SV University, Tirupati. presently working as a Professor in Department of Electrical and Electronics Engineering, Sri Venkateswara University College of Engineering, SV University, Tirupati, Andhrapradesh, India-517502.